Advanced Fracture Modeling for Cuttings Re-injection

Jorge Garzon, Matias Zielonka, Kevin H. Searles and Pablo Sanz

ExxonMobil Upstream Research Company

22777 Springwoods Village Parkway, Houston, TX 77389

Abstract: *An environmentally friendly and cost-effective method for waste-disposal operations commonly used worldwide in the oil and gas industry is known as Cuttings Re-Injection (CRI). It consists of injecting drill cuttings into a suitable geological formation through one or more hydraulically-induced fractures. In this paper, some case studies assessing the risks associated with CRI are introduced using recently co-developed capabilities in Abaqus Standard for simulating fully-coupled hydraulic fracturing. Finite element models (FEM) are constructed using material properties and in situ stress state based on well log information. Furthermore, models are calibrated using data from actual field injection tests.*

This new 3D simulation capability in Abaqus Standard overcomes some of the limitations of traditional tools and gives engineers an opportunity to assess the impact of planned CRI operations on predicted fracture geometry and pore pressure changes. These variables are very important in understanding risk to formation top seal integrity and possible interaction with pre-existing discontinuities, both of which may lead to loss of fluid containment and non-compliance with environmental regulations.

Keywords: *Cuttings re-injection, CRI, Hydraulic fracturing, Pore pressure, Injection, Geomechanics*

1. Introduction

In the late 1980s, the industry began large scale subterranean injection of slurrified drill cuttings in Alaska and the Gulf of Mexico [1]. At that time, the process of injecting was done open hole and most well-related wastes that could be rendered into slurry were injected for disposal. Other kinds of materials produced in the drilling process were considered as useful construction materials (sand and gravel). Currently, governmental regulations concerning injection are taken into account although they may vary from country to country. In general, disposal of material wastes related to drilling, completion and production operations such as oily cuttings, waste drilling fluid, oily water, waste brines and other liquids, are covered by governmental regulation and are candidates for downhole injection. Some other wastes associated with well operations (e.g. waste fuels, rig debris) classified as industrial wastes may not be injected in some jurisdictions.

There are different approaches to managing drill cuttings waste. For example, common methods used offshore include cuttings dehydration, thermal or mechanical treatment with onsite cuttings processing, or shipping to shore for processing. Each method has its application under different circumstances, but downhole injection can be the preferred method when feasible and is appropriate due to several advantages:

1) No transportation risks; it does not rely on shipment of wastes, spill contamination and weather related risks offshore
2) No future clean-up liabilities; when properly injected, waste is permanently immobilized in subterranean formations with little risk of water contamination
3) No limit to location; this type of treatment can be performed on-shore and offshore
4) Favorable economics; costs can become lower in the right environment.

Cuttings Re-Injection (CRI) is a common practice in many regions including, North Sea, Gulf of Mexico, Alaska, offshore California, Sakhalin Island and Eastern Canada. An ideal CRI project goes through a well-planned and integrated process to guarantee adequate barriers to prevent potential hazards (e.g., surface broaching). A detailed study (pre-screening and during any injection program) is necessary to determine whether the geological setting is suitable to prevent escape of waste. Some of the essential details needed include fracture size versus injection volume and pressure and these can be obtained more accurately using advanced simulations. The successful progress of an injection project can be evaluated with daily pressure monitoring and model calibration (updated simulations). Guo et al. [2] described a successful example of integrating all these components to estimate storage capacity and assess the operational integrity of disposal wells.

CRI modeling requires a pseudo three-dimensional or, even better, a three-dimensional fully-coupled hydraulic fracturing simulator to predict the geometry of injection induced fractures and evaluate the risk of a broaching situation. Some developed software called MFrac commonly used in industry [3]. Although this pseudo three-dimensional software is capable of modeling CRI, it has these limitations: simulation of a single fracture, fixed number of batches, fracture geometry fixed to an ellipse, ignoring stress buildup due to solids accumulation and no information about pore pressure changes inside the rock. Despite these limitations, this software has proven useful to estimate conservative bounds of the disposal domain [4-6]. The general consensus in the industry is that multiple parallel fractures grow due to the injected cuttings and it is conservative to assume that all the volume will propagate one long fracture. ExxonMobil Upstream Research Company (URC) is working with SIMULIA® to overcome some of these limitations with recently co-developed, three-dimensional, fully-coupled hydraulic fracturing capabilities for Abaqus Standard.

In this paper, two case studies assessing the risk associated with CRI are introduced using the co-developed capabilities. All finite element (FE) models are constructed using material properties

and in situ stress state based on well log information. In addition, models are calibrated using data from injection tests performed in the field.
Results from these simulations give an estimate not only of fracture geometry but also pore pressures changes along the fracture and within the surrounding rock. This information is essential to minimize the risk associated with breaching top seals and possible fracture intersections or reactivation of any neighboring faults. Engineers need to ensure fluid containment and compliance with environmental regulations.

2. Model set-up: Material Properties and FE Mesh

Finite element analysis (FEA) has been used for more than 40 years to simulate the mechanical behavior of materials. It is a numerical technique for finding an approximate solution and it consists of partitioning a problem into simpler parts, called elements. Theoretically speaking, if these elements are infinitely small the approximation reaches the true solution of the problem, but in practice the size of the elements depends on the computational power and simulation time. Therefore, the numbers of elements and their size have to be such that a good approximation of the solution can be obtained in a reasonable time.

CRI problems tend to have very large domains extending over 1 km in all directions, and good approximations for fracture problems require very small elements (less than 0.1% of the crack size). This makes the creation of these types of models very challenging. In the following models, multi-point constraints are used to refine close to the fracture plane and maintain continuity between elements.

Material properties and initial conditions come from a rock physics model (RPM) created based on well log data (e.g. sonic, gamma ray, density, etc.). Some estimates of both include Young's modulus, Poisson's ratio, porosity, permeability, fracture toughness, pore pressure, horizontal and vertical initial stress, etc. The resolution of the well log data is much higher than the discretization of the FEA model and thus, zoning and up-scaling methods are necessary to accurately assign representative values to each element in the model. In this section the material properties and initial conditions for two case studies are presented.

2.1 Case Study 1

In this model, a rock formation with dimensions 800x800x900 meters, as shown in Figure 2.1, is simulated. The FE mesh created is only for half of the problem since a symmetry plane is considered. The injection location is at 2,370 m TVD. The model consists of 641,000 hexahedral elements with the smallest element having a size of 1.2 m.

The model has been discretized by 46 material layers with a higher resolution close to the injection location. After creating the RPM based on the well log information, all material properties and initial conditions have been up-scaled to the FE material layers as shown in Figure 2.2. The colored rectangles correspond to the largest element size on the FE layer, the dark blue line is the data at the well log resolution and the yellow line corresponds to the up-scaled data. Notice that a constant value of the data is assigned to each FE layer.

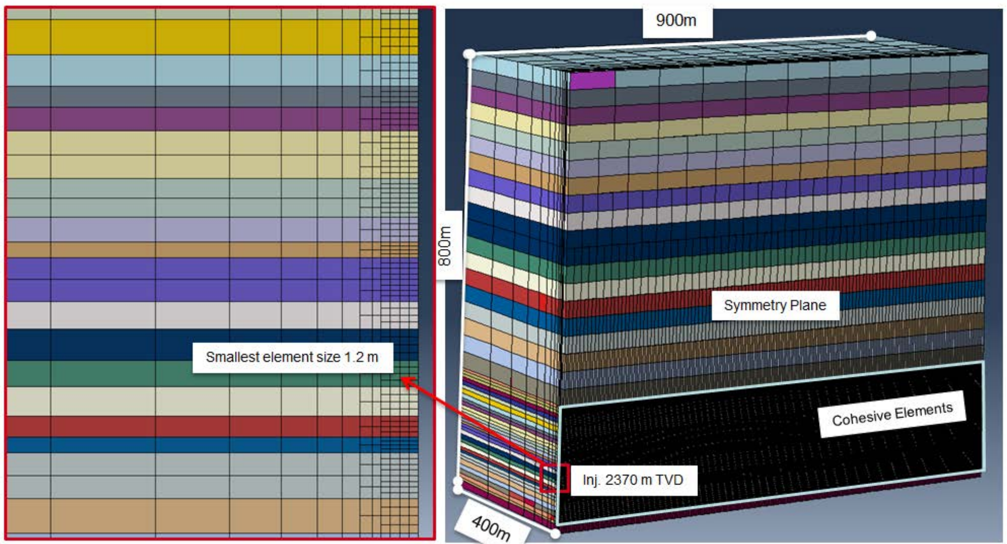

Figure 2.1. Case Study 1: Finite Element Mesh. Symmetric model with 46 different material layers for CRI injection.

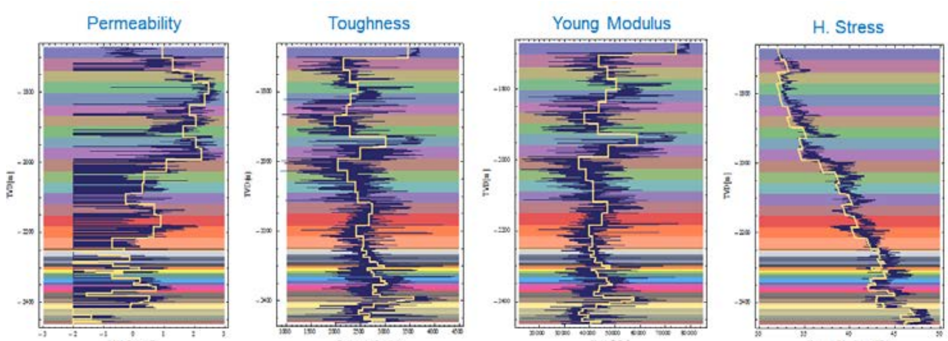

Figure 2.2. Case Study 1: Material properties and initial conditions up-scaled to 46 finite element layers.

Young's modulus, Poison's ratio, initial stress and pore pressures are inserted directly into the input file, permeability is used to compute hydraulic conductivity which is the value required for the soils analysis. Additional material information needed for this type of model is the fluid viscosity.

2.2 Case Study 2

The dimensions of this problem are 1,900x1,055x1,300 meters as shown in Figure 2.3. Again, due to symmetry only half of the problem is simulated. The injection location is at 1,128 m TVD. The model consists of 221,000 hexahedral elements with the smallest element having a size of 2.7 m.

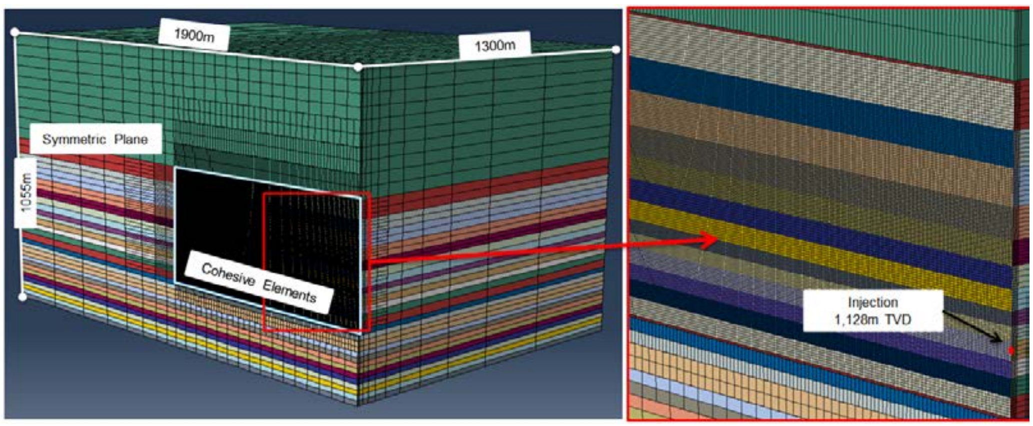

Figure 2.3. Case Study 2: Finite Element Mesh. Symmetric model with 26 different material layers for CRI injection.

This model has 31 material layers. A RPM was created based on the well log information and all material properties and initial conditions have been up-scaled to the FE material layers as shown in Figure 2.4. Notice that the first layer in this model is very large compared to other layers. Since well log data was not available for that interval, constant values were assumed. Permeability in this problem is not well-known but the calibration exercise explained in the next section allows for adjusting to a value representative of the field conditions.

As done in previous example, Young's modulus, Poison's ratio, initial stress and pore pressures are inserted directly into the input file. Permeability and fluid viscosity are used to compute hydraulic conductivity. The CRI fluid considered has a viscosity expressed by Power-law constants of n=0.53 and k=0.028 lbs secn/ft2.

In this section, the creation of two finite element models was presented. Material properties and initial conditions prescribed at each element are derived from up-scaled rock physics models based on well log data. To ensure a correct representation of the field conditions, the FE models are calibrated using data from injection tests. This calibration process is described in the following section.

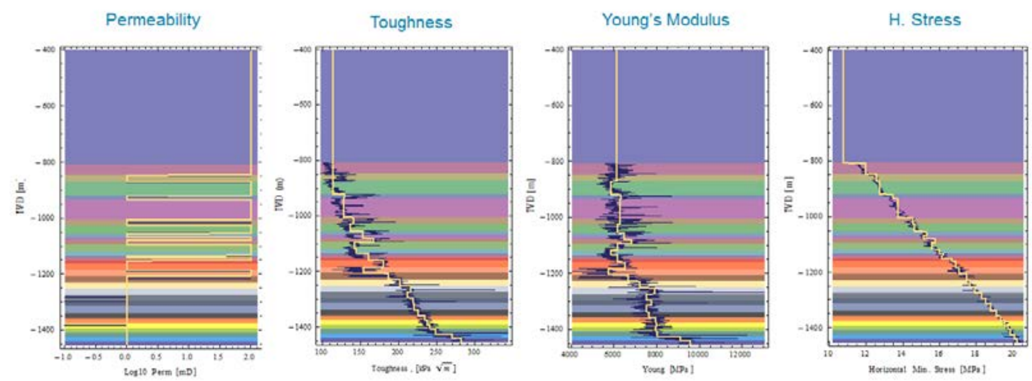

Figure 2.4. Case Study 2: Material properties and initial conditions up-scaled to 31 finite element layers.

3. Model Calibration

Rock physics models (RPM) were created for two study cases to obtain material properties and initial conditions. Although these RPMs have high resolution and tend to be a very accurate representation of the field conditions, the coarsening and up-scaling process may deteriorate the precision of the input data. Therefore, a calibration of the FE model is necessary to assure a good representation of the problem. In this section, calibration is done by simulating an actual injection test carried out in the field. Measured pressure data is recorded and used for comparison.

3.1 Case Study 1

In this example, an injection test of 216 minutes is simulated using the injection rate schedule provided from field operations as input. All other material properties and initial conditions remain as explained in the previous section, the injection fluid is sea water. The injection test consists of a ramped-up injection interval, a shut-in interval and a constant injection period.

The simulated injection pressure results are shown in Figure 3.1. The gray line is the injection rate schedule (input), the red line corresponds to pressure measured at the field and the green line is inlet pressure output from the FE simulation. The field data is measured at surface conditions, but it has been adjusted to reflect flowing bottom-hole conditions by considering hydrostatic pressure and frictional losses. This allows for a more direct comparison with the FE simulation output. The location of the pressure output in the FE simulation is taken at the injection point inside the fracture (depth 2,370 m TVD). Additionally, snapshots with a contour representing the fracture opening (units are meters) at specific injection times are shown.

In general, FE results show a very good match to the pressure measured at the field. A small difference is noticed at the time interval 30-35 min. This difference is due to the time that it takes to completely fill up the pipe with the injection fluid. This is not simulated at the moment and it is assumed that the pipe is 100% filled before injection starts. Therefore, the breakdown pressure for the FE simulation is reached at an earlier time.

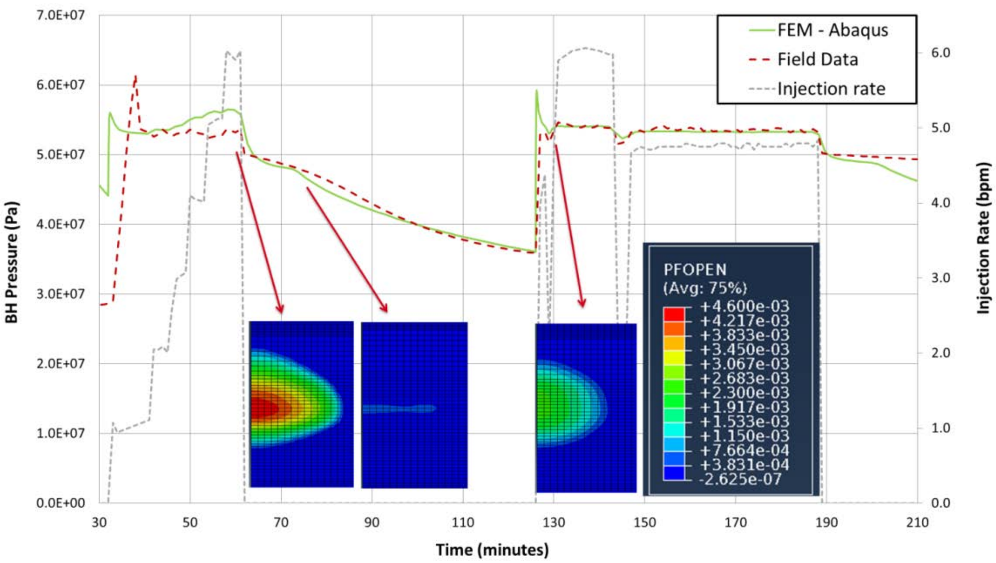

Figure 3.1. Case Study 1: Pressure results from the injection test and fracture opening at 3 different injection times.

At approximately 75 minutes after fracture closure (shut-in), the rate of inlet pressure decay becomes dependent on formation permeability (transition from bi-linear to radial flow). Here, the match between measured and simulated pressures suggests an accurate representation of rock permeability used in the model. This type of post-closure response cannot be obtained in a pseudo three-dimensional simulator, such as MFrac for example. After the fracture closes, this type of simulator cannot perform computations to consider the pore pressure diffusion into the surrounding rock formation. In addition, the FE results demonstrate a fairly good match with measured propagation pressure. This provides further assurance that estimation of the initial conditions considered in the model are reasonable.

For the aforementioned calibration example, no adjustments of material properties or initial conditions were needed to obtain a good match to the field behavior. This injection test simulation guarantees that the FE model has a good representation of the field characteristics and can serve as a good approximation of the true behavior.

3.2 Case Study 2

In the previous case study, the measured surface injection pressure was corrected to flowing bottom hole conditions by considering hydrostatic pressure and frictional losses. This was done to facilitate comparing measured pressure to simulated inlet pressure at the modeled injection location. In this case study, pipe elements are used to simulate Bernoulli fluid flow from the surface to the injection location. This allows making a straight-forward comparison to the pressure results at the surface without having to perform any manual computations. Figure 3.2 shows the FE model with the pipe elements. The contour corresponds to initial pressure (hydrostatic). Note that pressure is zero at the surface (0.0 m TVD).

The injection test in this example consists of 50 minutes of injection duration at 4 bpm and 50 minutes of shut-in time. All material properties and initial conditions are the same as explained in the previous section. A sensitivity study is also conducted for permeability since it is an unknown in the problem. The injection fluid is assumed to be seawater.

For this particular example, the actual field injection test was carried out following 300 days of injection, thus a fracture should have existed by the time of the test. To simulate that current state of the rock formation, a set of cohesive elements close to the injection location was initialized to represent existing damage. These elements are colored red in Figure 3.2. This initial damage may not be representative of the actual fracture in the field, but it is large enough to dissipate all fluid injected during this short injection test. The key for this simulation is to re-open a preexisting fracture without inducing additional fracture propagation.

Results of this simulation are shown in Figure 3.3. The gray line is the injection rate schedule (input), the red line corresponds to the measured surface pressure, the green and blue lines are the inlet pressure outputs from the FE simulation for a 50 mD and 30 mD rock permeability assumption, respectively. Both FE simulation pressure results are output at the pipe inlet (0.0m TVD). These results can be compared directly to the field data measured at the surface, because the pipe elements solve for hydrostatic pressure and frictional losses during the simulation. Also shown are snapshots of a contour representing the fracture opening (units are meters) at specific injection times for the 30 mD assumption.

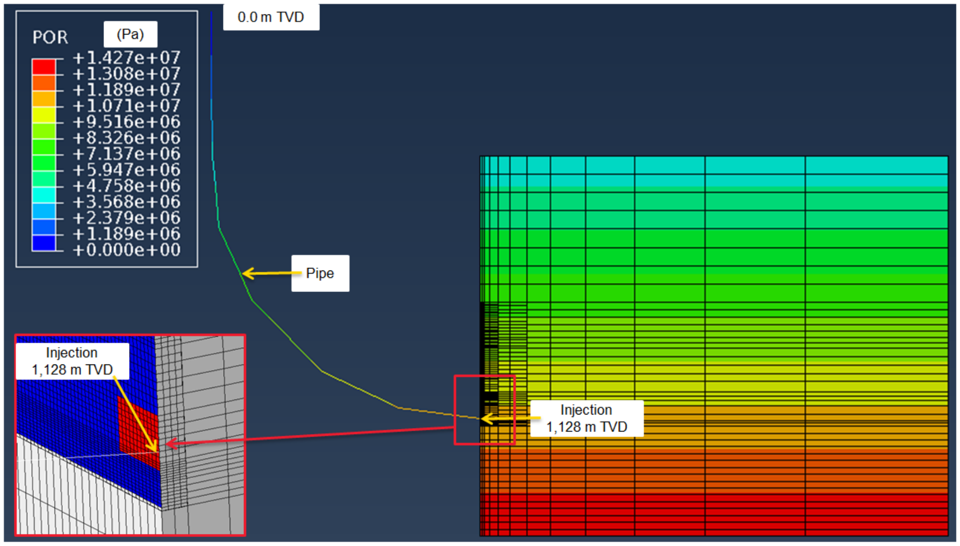

Figure 3.2. Case Study 2: Initial pressure contour and description of pipe elements and trajectory to injection location.

In comparison to the results from the prior case study, the FE results for this case are not as accurate. This is mainly due to the inadequate discretization of the rock permeability. Although this important rock characteristic is unknown, the results suggest that an assumption between 30 to 50 mD is sufficient to obtain a similar behavior as observed in the field.

The difficulty in this particular case study stems from the lack of information regarding rock permeability. However, this calibration exercise is still very useful in finding discrete values that seem to be representative of the field behavior. This helps to assure that the FE model is a good representation of the field characteristic and serves as a good approximation of the true behavior.

4. Results and Conclusions

A calibrated fully-coupled FE model with reliable material properties and initial conditions is a useful tool to investigate different scenarios for CRI. The FE model can predict crack surface geometry, pressure changes at the fracture inlet and pressure diffusion into the surrounding rock. This helps to assess the risk of compromising the integrity of the formation top seal and possibly the reactivation and intersection of any pre-existing discontinuities (fracture and faults), both of which may lead to loss of fluid containment and non-compliance with environmental regulations.

In this section, results for a CRI simulation are presented for the two study cases calibrated in the previous section. A 100 day-injection duration is carried out for both examples. Figure 4.1 shows the injection rate schedule which consists of 17 cycles of single-day injection and 5 days of shut-in time.

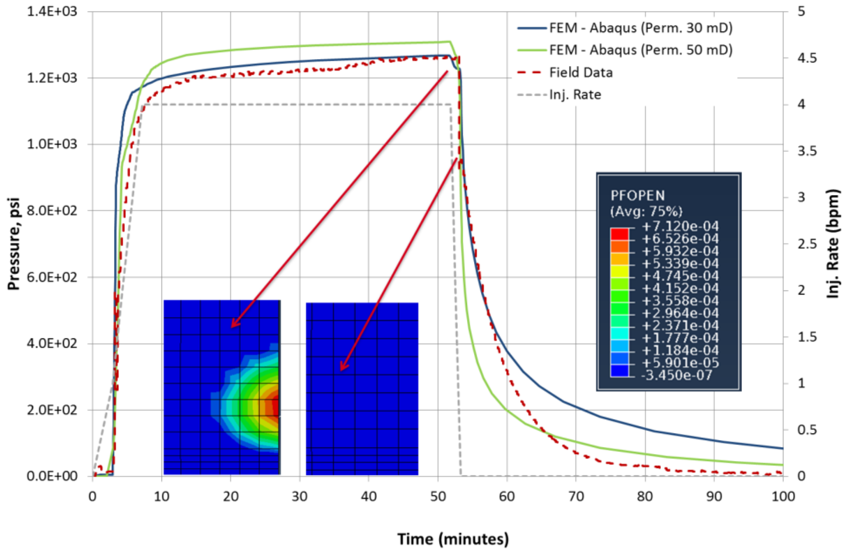

Figure 3.3. Case Study 2: Pressure results from injection test and fracture opening at 2 different injection times (30 mD assumption); units are meters.

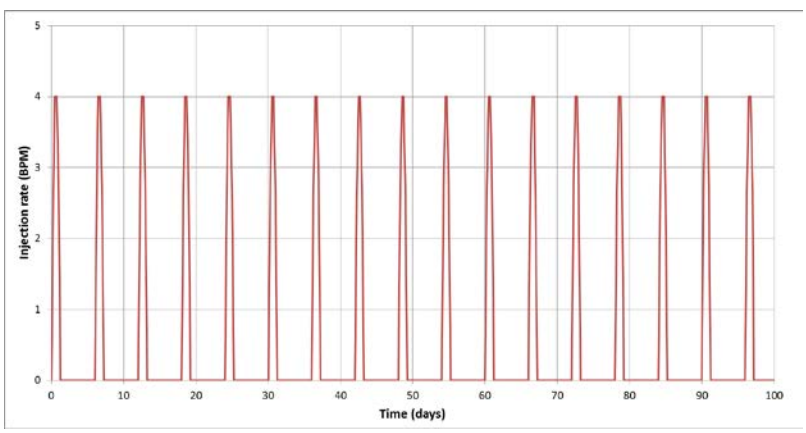

Figure 4.1. Injection rate schedule used for CRI simulation.

4.1 Case Study 1

The material properties and initial conditions remain unchanged from the previous section. The injection fluid is assumed to be sea water to facilitate a comparison with Case Study 2.

Simulation results show that the crack opens and propagates during injection cycles and closes completely during the shut-in period. Figure 4.2 shows the evolution of the crack surface at different days and contours correspond to the fracture opening width. The bottom right figure illustrates the fracture damage variable after 97 days of injection. This damage variable represents the rock that was damaged or fractured during the injection but may not be currently open. In this example, most of the propagation of the fracture occurs during the early cycles, while re-opening of the preexisting fracture dominates the later part of the injection.

After 100 days of sea water injection, the predicted fracture length is 52 m and the height is 34 m.

Another important insight obtained from this FE simulation is the pore pressure changes inside the fracture and in the formation away from the fracture. Figure 4.3 shows the pore pressure evolution for two locations: i) at the injection point (2,370 m TVD) and ii) 70 m perpendicular to the fracture plane (inside the rock). The increase in pore pressure inside the fracture is substantial during injection (80 MPa) and very similar after the first cycle. The decrease of pore pressure also occurs rapidly; the pressure drops about 25 MPa in less than 2 days after shut-in. As expected, the variations on the pore pressure are less significant away from the fracture. Figure 4.3 shows that the pore pressure 70 m from the injection location experience minor changes.

Figure 4.4 shows two contour plots for pore pressure change in terms of percentage from its initial value after 97 days of injection. Contour a) shows pore pressure changes on an isometric view of the problem, notice that fracture propagates in the YZ plane. Pore pressure changes are more significant close to the fracture and thus more significant pore pressure changes are observed on the fracture plane. Contour b) shows a XZ cut-in plane at the injection point (2,370 m TVD). This gives a better view of what happens inside the rock away from the fracture. The pore pressure change at a radius of ~65 m around the fracture is insignificant.

4.2 Case Study 2

In this example, material properties and initial conditions remain the same as explained in previous sections. In order to capture the contrast in permeability between element layers representing sand and shale, permeability of 500 mD and 5 mD are assumed as upper and lower bounds, respectively. The fluid injected is simulated as a non-Newtonian slurry with viscosity given by the Power-law constants n=0.53 and k=0.028 lbs secn/ft2.

Similarly to previous case, the crack opens and propagates during injection cycles and closes completely during the shut-in period. Figure 4.5 shows the complex evolution of the fracture geometry during injection. Each injection cycle shows a different behavior. Locations that were fractured in a previous cycle may not be re-opened in the current steps; instead fracture propagation may occur elsewhere. Thus, fracture damage is a good indicator of the different paths the fluid took during fracturing. In this example, fracture propagation is more significant in length than height when compared to previous case. Even though it propagates upwards, there are barriers that do not allow an important propagation towards the surface.

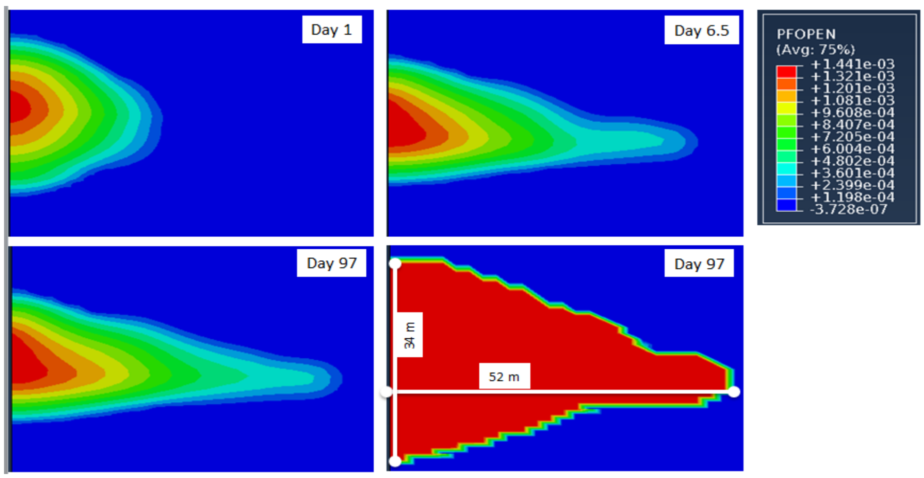

Figure 4.2. Case Study 1: Crack surface evolution, fracture opening and final damage state.

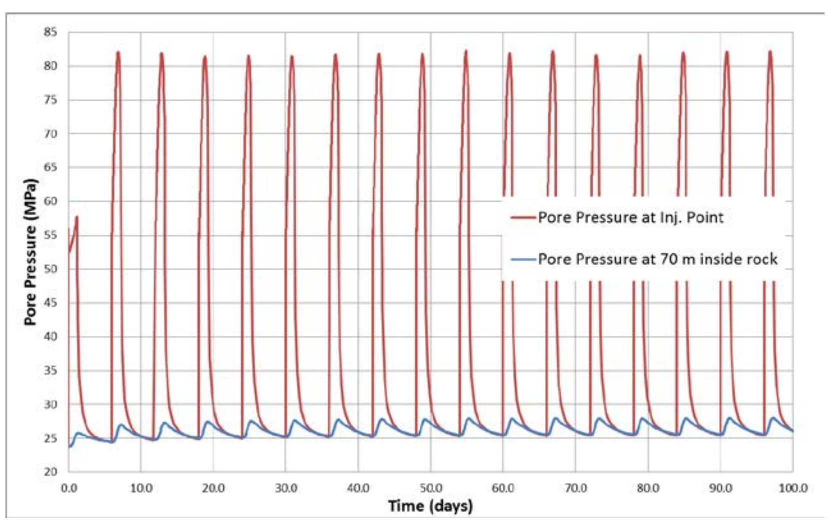

Figure 4.3. Case Study 1: Pore pressure evolution at injection location (red) and at 70 m from injection location (blue).

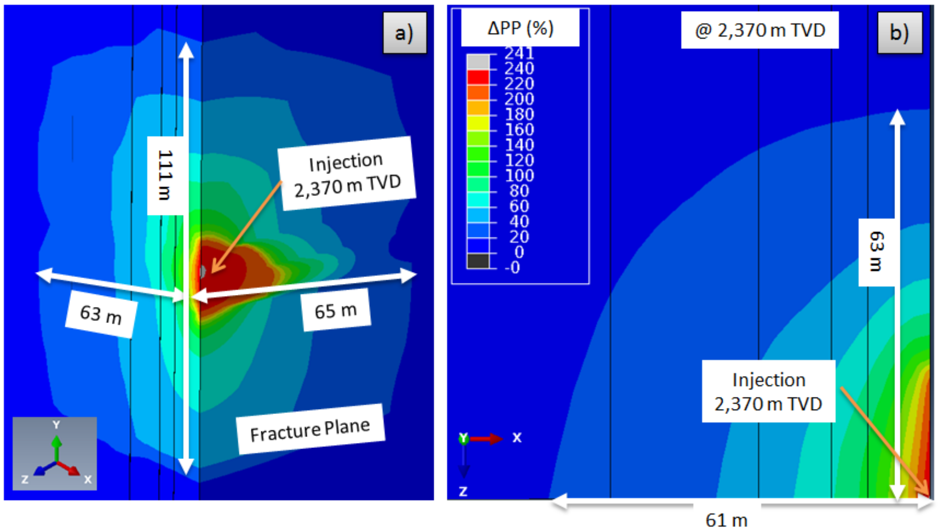

Figure 4.4. Case Study 1: Pore pressure changes (%) after 97 days of injection (just after last injection cycle); a) Isometric view, b) Cut-in plane at depth 2,370 m TVD. The fracture propagates on the YZ plane.

Figure 4.6 shows the pore pressure evolution at the injection point (1,128 TVD) and 90 m away from the fracture plane. Larger time steps were utilized in this simulation to save computer memory. For this reason, the pore pressure evolution curves are not as smooth as in the previous example.

The increase and decrease of pore pressure is significant close to the fracture. As you move away from the fracture, the magnitude and fluctuation of the pore pressure rapidly decreases. Figure 4.7 shows two contour plots for pore pressure change in terms of percentage from its initial value after 97 days of injection. Contour a) shows on an isometric view that pore pressure changes are more significant near the fracture. Contour b) shows a XZ cut-in plane at the injection point (1,128 m TVD). The pore pressure change is insignificant at a radius of ~300 m around the fracture.

4.3 Conclusions

The size of the fracture in Case Study 1 is small compared to the fracture in Case Study 2. This is mainly driven by the differences in the rock permeability and fluid viscosity. While sea water is injected in the first case, viscous slurry is injected in the second example. Hydraulic conductivity is the rate of flow through a cross-sectional area, and is a function of permeability, fluid density and viscosity. The hydraulic conductivity of case 1 is about 2 orders of magnitude greater than in case 2. This means that fluid can travel quicker in the first case. This can also be seen in the pore pressure behavior, in case 1 pore pressure changes occur rapidly and it stabilizes in a few days.

Another observation is that pore pressure changes are greater in case 1 because the injection point is at a deeper location, thus a higher compression has to be overcome to open a fracture.

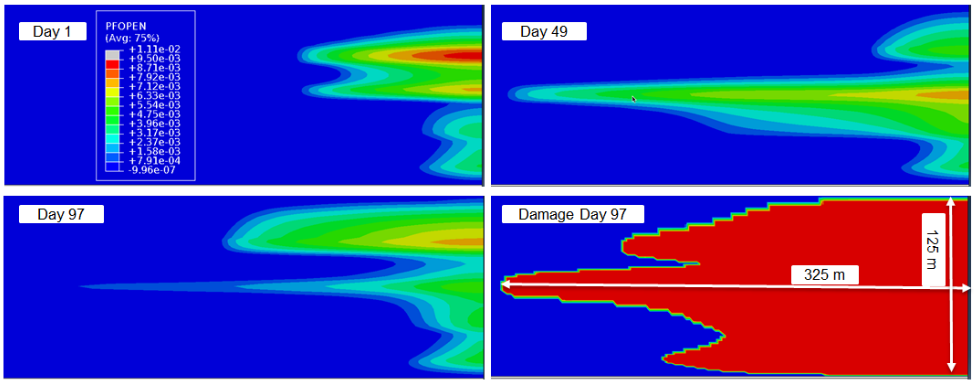

Figure 4.5. Case Study 2: Crack surface evolution, fracture opening and final damage state.

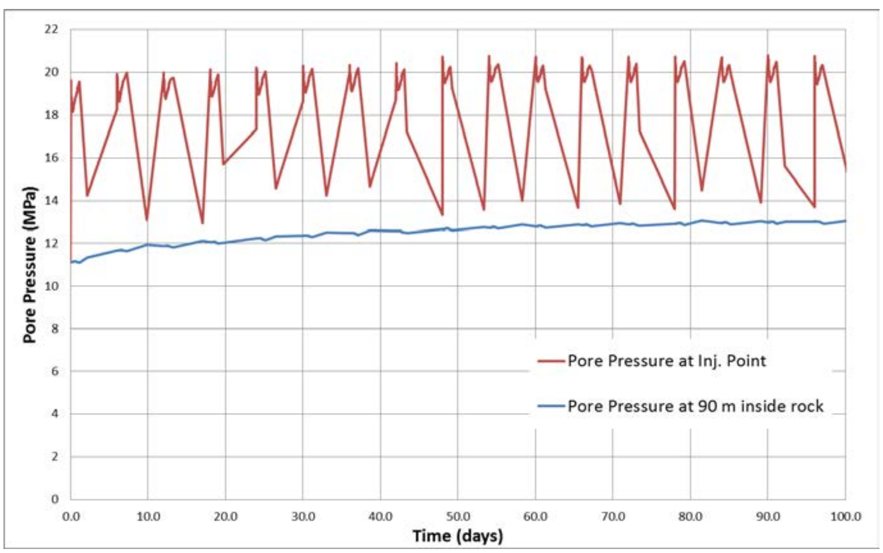

Figure 4.6. Case Study 2; Pore Pressure evolution at injection location (red) and at 90 m from injection location (blue).

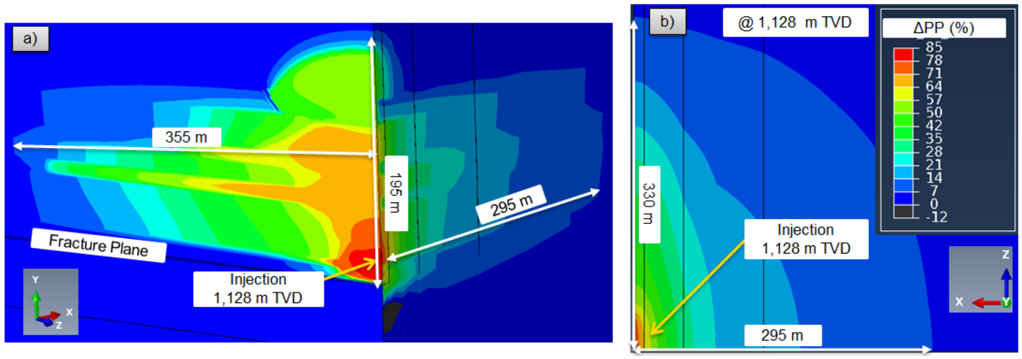

Figure 4.7. Case Study 2: Contours showing pore pressure changes after 97 days of injection (just after last injection cycle); a) Isometric view, b) Cut-in plane at depth 1,128 m TVD.

Pore pressure and fracture geometry have been predicted for two CRI examples. Height and length are important insights that assure fluid containment. Also contours of pore pressure change have been presented to show the extent of perturbation of the formation rock. This can be used as an overview of the trajectory of the injected fluid and amount of perturbation in terms of pressure. If any important geologic features exist (e.g. pre-existing faults) within the region of interest, more complex models can be created to understand the consequence of perturbing the pressures and stresses at those particular features. This is future work and it is beyond the extent of this paper.

In this study filter cake buildup has not been considered. Filter cake is understood as a barrier between the fracture and the rock formation, that reduces the rate (leak-off) at which the fracturing fluid flows. This can be easily added to the CRI simulation by means of a user subroutine.

None of the current semi-analytical fracture modeling tools predicts injection-induced hydraulic fracturing with a fully coupled 3D formulation. Enhanced fracture modeling capabilities are needed to address increasingly complex business questions. More accurate models would lead to optimized well designs, and would assist in acquiring permits for cuttings disposal operations from regulatory bodies and further reduce risk of environmental impact.

5. Acknowledgments

The authors would like to thank ExxonMobil Upstream Research Company for permission to publish this work.

6. Bibliography

1. Guo, Q., Abou-Sayed, A. S., and Egel, H. R., "Feeling the Pulse of Drill Cuttings Injection Wells - A Case Study of Simulation, Monitoring and Verification in Alaska". SPE Journal, 2007, 458-467.
2. Hofmann, Hannes, Babadagli and Zimmermann, G. “Hot water generation for oil sands processing from enhanced geothermal systems: Process simulation for different hydraulic fracturing scenarios”. *Applied Energy*, 113, 2014, 524-547.
3. Malachosky, E. and Lantero, DM., “Disposal and Reclamation of Drilling Waste”, U.S. Patent No. 4,942,929 July 4, 1990.
4. Meyer, B.R. "Three-Dimensional Hydraulic Fracturing Simulation on Personal Computers: Theory and Comparison Studies". SPE 19329, 1989, 1-18.
5. van der Hoorn, K., Heijnen, L.J., Gankema, M.E. and Nitters, G., “Hydraulic Fracturing In Limestone: A Case Study of Two EGS Projects in The Netherlands", PROCEEDINGS, Thirty-Seventh Workshop on Geothermal Reservoir Engineering, January 30, 2012
6. Warpinski, N.R., Moschovidis, Z.A, Parker, C.D., and Abou-Sayed, I.S., "Comparison Study of Hydraulic Fracturing Models - Test Case: GRI Staged Field Experiment No. 3". SPE Production & Facilities, 1994. 7-18.